Multichannel dosemeter and Al2O3:C optically stimulated luminescence fibre sensors for use in radiation therapy: evaluation with electron beams

Sylvain Magne, J. Bordy, L. de Carlan, A. Isambert, A. Bridier, P. Ferdinand, J. Barthe, Laureline Auger

Radiation Protection Dosimetry (2008), Vol. 131, No. 1, pp. 93–99 doi:10.1093/rpd/ncn226
Advance Access publication 30 August 2008

MULTICHANNEL DOSEMETER AND Al_2O_3:C OPTICALLY STIMULATED LUMINESCENCE FIBRE SENSORS FOR USE IN RADIATION THERAPY: EVALUATION WITH ELECTRON BEAMS

S. Magne[1,*], L. Auger[1], J. M. Bordy[2], L. de Carlan[2], A. Isambert[3], A. Bridier[3], P. Ferdinand[1] and J. Barthe[4]
[1]CEA, LIST, Laboratoire de Mesures Optiques, F-91191 Gif-sur-Yvette, France
[2]CEA, LIST, Laboratoire National Henri Becquerel, F-91191 Gif-sur-Yvette, France
[3]Institut Gustave Roussy, Service de Physique, 39 rue Camille Desmoulins, F-94805 Villejuif, France
[4]CEA, LIST, Département des Technologies du Capteur et du Signal, F-91191 Gif-sur-Yvette, France

This article proposes an innovative multichannel optically stimulated luminescence (OSL) dosemeter for on-line *in vivo* dose verification in radiation therapy. OSL fibre sensors incorporating small Al_2O_3:C fibre crystals (TLD_{500}) have been tested with an X-ray generator. A reproducible readout procedure should reduce the fading-induced uncertainty ($\sim -1\%$ per decade). OSL readouts are temperature-dependent [$\sim 0.3\%\ K^{-1}$ when OSL stimulation is performed at the same temperature as irradiation; $\sim 0.16\%\ K^{-1}$ after thermalisation (20°C)]. Sensor calibration and depth–dose measurements with electron beams have been performed with a Saturne 43 linear accelerator in reference conditions at CEA-LNHB (ionising radiation reference laboratory in France). Predosed OSL sensors show a good repeatability in multichannel operation and independence versus electron energy in the range (9, 18 MeV). The difference between absorbed doses measured by OSL and an ionisation chamber were within $\pm 0.9\%$ (for a dose of about 1 Gy) despite a sublinear calibration curve.

INTRODUCTION

Today, about 60% of all cancer patients are treated totally or partially by radiation therapy (RT). Most RT treatments involve photon and electron beams delivered by linear accelerators (LINACs). The so-called conformal RT and intensity-modulated RT (IMRT) improve the conformity of the dose distribution to the tumour, thus delivering a reduced dose to the surrounding healthy tissues and critical organs. In return, it brings additional complexity and processing time in the dosimetry because of high-dose gradients and more complex ballistics.

Treatment planning systems (TPS) are used to plan the treatment. Severe accidents in radiotherapy have been associated with the incorrect use of TPS or false dose measurement during its commissioning. *In vivo* dosimetry is therefore becoming a legal requirement in France in order to provide a true check of the absorbed dose actually delivered. According to the Code of Practice (CoP) IAEA TRS-398[(1)], the difference between planned and delivered doses must remain typically between 2 and 3%. If the difference exceeds 5%, the reasons for discrepancy must be investigated and the patient's treatment must not be initiated.

In vivo dosimetry is traditionally provided by thermoluminescent dosemeters (TLDs), metal-oxide semiconductor field-effect transistors (MOSFETs) or PN-junction-type diodes. However, *in vivo* optically stimulated luminescence (OSL) dosimetry with Al_2O_3:C crystals is recently gaining acceptance in the medical community[(2–5)]. As a matter of fact, dosimetric-grade alumina crystals (grown in reducing atmosphere in the presence of carbon) provide a lot of advantages [high sensitivity, large dynamic range, small fading at room temperature, low Z ($\sim$11), etc.]. Recent clinical investigations were performed with InLight™ Dot dosemeters (associated with the microStar reader) or Luxel™ film dosemeters, collected after irradiation and sent to Landauer Inc. (Glenwood, IL, USA) for readout. A readout does not bleach the film. It may be stored and read at a later date.

However, in clinical conditions, medical physicists intend to save time in collection procedures and have access to the absorbed dose data immediately after treatment in order to provide suitable remedial action in case of abnormal dose delivery. The real-time monitoring of the cumulated doses may also be mandatory for specific treatments (*e.g.* total body irradiation) and may be obtained from real-time OSL or radioluminescence (RL) of Al_2O_3:C crystals.

For this purpose, several research groups have investigated fibre-sensing solutions for on-line remote dose measurement in RT, mostly with Al_2O_3:C crystals[(6–9)]. The multisensor capability of our OSL fibre reader for the purpose of cost-effectiveness (improvement of the cost/sensor figure)[(9)] and easier data acquisition and archiving

*Corresponding author: sylvain.magne@cea.fr

are the main innovations described in this paper. Furthermore, the RL signal may also be measured during irradiation from one or multiple sensors (time-sampling by the optical switch). The OSL/RL sensor, linked to a fibre cable, thus provides a real-time estimation of the dose rate (or cumulated dose) during treatment and on-line estimation of the dose after treatment. The objective is to provide an accurate, cost-effective, efficient and reliable *in vivo* dosimetry to fulfil the quality assurance in RT while maintaining operational costs at a reasonable level.

Al_2O_3:C OSL fibre sensors are radiation-transparent (made with polymers) and do not involve metallic wires (silica or polymer fibres). They are compatible with *in vivo* applications [small (mm size)], non-toxic, chemically inert and sterilisable), electromagnetic-immune and exhibit low energy and angular dependencies. Finally, in the context of an ever-increasing complexity of the radiation treatments, the purpose of such sensors is also to save time in calibration and maintenance, taking advantage of both radiation hardness of the sensor (long lifetime) and material stability relaxing the need for frequent recalibrations.

This work is done within the European Project MAESTRO, dedicated to the development of technologies and treatment techniques in RT. It is managed by the CEA LIST and involves several cancer research institutes and hospitals, among which the Institut Gustave Roussy (IGR) is one centre of expertise.

OPTICALLY STIMULATED LUMINESCENCE SYSTEM

The scheme of the multichannel OSL reader is based on a previous work[10,11] and is depicted in Figure 1.

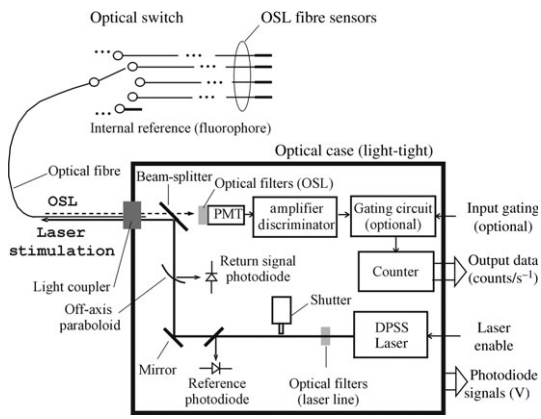

Figure 1. Basic scheme of the multichannel optically stimulated luminescence reader of the CEA LIST.

The OSL reader is built on a 19-inch enclosure (6U) that includes a 16-channel optical fibre switch actuated by a stepper motor, an optical case and power/USB electronics[9]. The OSL reader is linked to a laptop by an USB connection (Universal Serial Bus) and handled through dedicated software written in LabView (National Instruments Corp., www.ni.com). During experiments with LINACs, the OSL reader is located in a control room (next to the irradiation room) and fibre cables run through the wall (length: 28 m).

An OSL fibre sensor consists of an optical fibre cable with an SMA connector (Subminiature A) at one end and a moulded cylindrical epoxy head ($Ø = 6$ mm) at the other. The head is rigidly fixed onto the cable extremity, protects the crystal ($Ø =$ 1 mm, 1 mm long) affixed near the end of a silica fibre ($Ø = 0.6$ mm) and provides a stable coupling of light. TLD_{500} alumina fibre crystals purchased from Ural State Technical University (Ekaterinburg, Russia) were used. The sensors exhibit circular symmetry along the fibre/crystal axis.

RL decays slowly after each LINAC pulse (several microsecond duration). A gating circuit may be inserted between the amplifier-discriminator and the counter (Figure 1) in order to discriminate in time RL versus Cerenkov perturbations from the fibre ('stem effect').

After irradiation, each OSL sensor is remotely stimulated using a continuous wave (CW) diode-pumped solid-state (DPSS) laser (at 532 nm, 200 mW) and bleached for a next use. The reader works in the CW mode (*i.e.* CW-OSL). The OSL stimulation is triggered by an electromagnetic shutter once the switch has moved from its reference position to the selected output. The OSL (at 410 nm) is then collected by the optical fibre, separated by a dichroic beam-splitter, filtered by a pack of Schott BG4/CVI CPAB505 filters and eventually detected by a photomultiplier (PM Electron Tubes, 9111B) in photon-counting mode. For a dose of 2 Gy, the error due to counter dead time (20 ns) is about 0.2%. To avoid deleterious effect over linearity (at high dose), the raw PM signal is corrected for dead time prior to calculations. Then, the background signal is averaged from the latest portion of the OSL signal and subtracted from the raw signal. The background is due to dark counts in the PM tube, imperfect filtering of the laser light and also fluorescence of the OSL crystal [metal impurities (especially Cr^{3+}) and deep-trap charges]. The corrected signal is then integrated and multiplied by a calibration coefficient to provide the absorbed dose. The error in OSL measurement is due to counting statistics ($1/\sqrt{N}$), background and temperature corrections. The integration usually runs until the OSL signal gets well below 0.1% of the integral. The bleaching time T_b depends mainly on laser

wavelength and power (the higher the laser power, the lower the T_b). To a lesser extent, it also depends on dose (the higher the dose, the higher the T_b). The integration time T_i is set identical to T_b in order to improve the reproducibility of OSL data (integration of the whole OSL decay curve). The time T_{bg} for background correction usually lasts for a few seconds. The OSL readout time ($T_r = T_b + T_{bg}$) is $\sim$20 s for a stimulation intensity of $\sim$25 mW mm^{-2}. For 12 sensors, T_r is 4 min, compatible with the treatment protocol. The limit in dose detection is $\sim$1 mGy.

The OSL response (Gy counts^{-1}) also depends on light transmission along the measurement chain (MC) from sensor to PM. Anomalies in light transmission or device operation are unlikely to occur with our OSL system but nevertheless, have to be taken seriously in a medical application. Consequently, a self-checkup of every critical device (laser, PM, optical switch) is done before use. Two photodiodes are inserted into the case. A reference photodiode monitors laser power and checks both the laser status and the reference for calibrating the MC. A fluorophore is placed inside the unit, located nearby a temperature sensor (Pt100), and connected to one output of the optical switch (15 outputs are left free for use). The MC calibration is obtained by dividing the PM output (counts s^{-1}) by the voltage of the reference photodiode.

Finally, the OSL dosemeter is safe when used properly. However, eye safety is also a matter of concern in case of abnormal use. The return signal photodiode monitors the laser signal brought back by the fibre and checks the integrity of the optical connection in order to switch the laser beam off in case of disconnection.

PRELIMINARY TESTS

Temperature and fading tests have been performed in the laboratory with an X-ray generator (80 keV) equipped with a dedicated lead cell rigidly fixed onto its mainframe. OSL sensors are placed inside a steel cylinder (Ø = 2 cm) that enables secure (tight) and reproducible positioning under the photon flux.

Temperature dependence of optically stimulated luminescence signal

The temperature of a dosemeter is likely to change depending on its placement on the patient's body. We investigated the temperature dependence of the RL and OSL measurements (Figure 2). An OSL sensor was permanently fixed inside the cylinder and stabilised in temperature. Irradiations were performed in $<$1 min and the sensor temperature is assumed to remain constant (due to thermal inertia of the cylinder). The temperature coefficient of the RL signal is $\sim$0.18% K^{-1}. The OSL temperature coefficient depends on whether OSL stimulation is done immediately after irradiation (*i.e.* at same temperature) or at room temperature (at 20°C) after sensor thermalisation. In the first case, the temperature coefficient is 0.3% K^{-1}, while it is 0.16% K^{-1} in the latter. Standard deviation of the data in Figure 2 is $\sim$1.2%. It is worse than the repeatability of the OSL reader probably because of temperature discrepancy ($\pm$0.5°C).

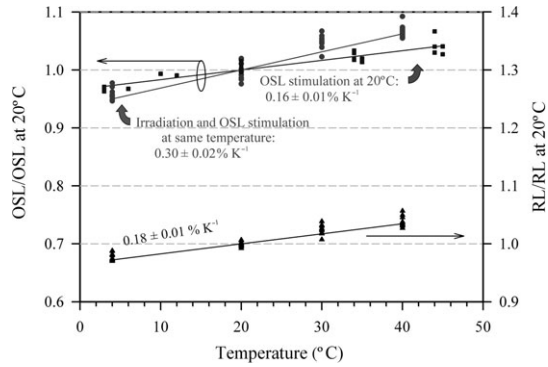

Figure 2. Change in optically stimulated luminescence and radioluminescence versus sensor temperature (normalised to mean values at 20°C).

The effect of temperature is less, but still cannot be neglected when performing on-line OSL dosimetry with TLD_{500} crystals. Under constant irradiation temperature and variable stimulation temperatures, Edmunds *et al.* also reported a wide range of OSL temperature coefficients depending on crystal type and integration time[12]. Jursinic did not observe any dependence versus irradiation temperature[3].

Fading of optically stimulated luminescence signal

The time delay between irradiation and OSL readout may change considerably according to the protocol of medical physicists. We conducted a fading test at 20°C for a constant irradiation time of 20 s (0.3 Gy). The time delay between the end of irradiation and onset of OSL readout was adjusted between 5 s and 2 h. In Figure 3, the OSL signal is plotted with respect to delay time and exhibits a small fading of about $-$1% per decade (order of magnitude in time).

Jursinic[3] observed a similar fading with InLight^{TM} dosemeters (Landauer) but also observed a transient signal that decays away in a few minutes after irradiation and recommends waiting at least 8 min to get a more stable readout. We did not observe any transient behaviour, indicating that prompt OSL readouts are possible with TLD_{500} alumina crystals.

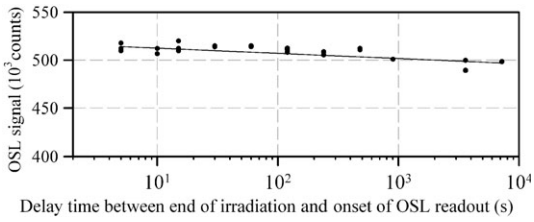

Figure 3. Fading of the optically stimulated luminescence (OSL) signal versus time delay between end of irradiation and onset of OSL readout.

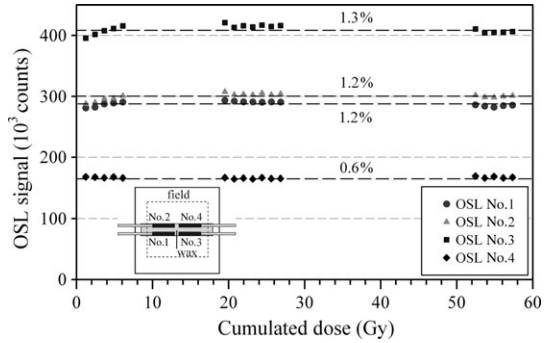

Figure 4. Repeatability test in multichannel operation with four optically stimulated luminescence sensors (inset shows the placement of sensors under the linear accelerator beam).

OPTICALLY STIMULATED LUMINESCENCE REPEATABILITY

Stability of the optically stimulated luminescence sensor's response versus dose

Preclinical tests have been performed with a Varian Clinac 2300 LINAC at IGR facilities [6 MV photon beam, field size (FS): $10 \times 10\,cm^2$, source-surface distance (SSD) = 1 m]. During these tests, we observed that both OSL and RL responses were changing with respect to cumulated dose ([0–100 Gy]) in the early use of the sensor. The RL decreased with cumulated dose, whereas the OSL increased in a significant proportion (~30%). This unstable behaviour is not due to sensor packaging (light coupling) as it would affect both signals in a similar way. It is due to the cumulative filling of deep traps that are not emptied by optical stimulation[13,14]. The sensor response eventually reaches a steady-state value versus cumulated dose once deep-traps are filled.

Repeatability in multichannel operation

Repeatability depends upon stability of both sensor and optical MC (particularly the optical switch). We have pre-irradiated four similar OSL sensors under increasing radiation predoses (^{60}Co source): no. 4: 250 Gy, no. 3: 500 Gy, no. 2: 750 Gy and no. 1: 1 kGy. Then, a repeatability test at constant dose fraction (1.2 Gy) was realised with those predosed sensors fixed on a polystyrene (PS) block and inserted into a groove filled with wax. The sensors were covered by a 2 cm-thick PS slab (at d_{max}). Figure 4 shows the repeatability of the OSL (between 0.6 and 1.3%) versus cumulated dose that demonstrates the stability of both predosed sensors and optical switch.

This result leads us to suppose that the minimum dose required is less than or about 250 Gy. The predose is done once and for all and would be included in the manufacturing process, prior to sensor calibration.

DEPTH–DOSE CURVES WITH ELECTRONS

Irradiation protocol

The treatment protocols with electron and photon beams are different, due to different interactions involved with matter. Since the sensors are placed onto the patient's skin, the protocol with electron beams involves a PMMA (plexiglass) bolus (whose diameter depends on electron energy) that shifts the depth of maximum dose onto the skin (small dose gradient).

Irradiations were performed at the CEA LIST LNHB (*Laboratoire National Henri Becquerel*), ionising radiation reference laboratory in France. Three reference energies were used (9, 12 and 18 MeV). Calibrations and depth–dose (DD) measurements were made with a Saturne 43 LINAC, according to the CoP TRS-398[1] that involves a water cube phantom (side length: 30 cm, wall thickness: 4 mm), FS = $10 \times 10\,cm^2$ and SSD = 1 m. The dose rate was 200 MU min^{-1} (2 Gy min^{-1}) at reference depth (z_{ref}).

A single OSL sensor (no. 3) was used for the experiment and connected to output no. 1 of the optical switch. The head of the OSL sensor was inserted and fixed into a PMMA tube (Ø = 13 mm) and immersed inside water. This sensor arrangement was placed vertically (transverse to the beam) and located on the horizontal central beam axis.

Calibration and energy dependence

Calibrations were made with an ionisation chamber (IC) calibrated by the CEA LIST LNHB. The sensor was placed at z_{ref} for all beams[1]. Top of Figure 5 shows the OSL data obtained for a dose up to 3 Gy. The calibration curves show sublinear behaviour typical of TLD_{500} alumina crystals[14]. Each curve may be simply modelled by a second-order

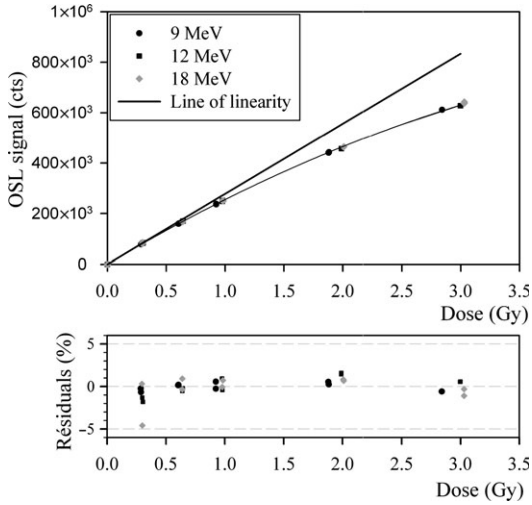

Figure 5. (Top) Optically stimulated luminescence (OSL) signal versus dose for the three electron energies (9, 12 and 18 MeV). (Bottom) Relative difference between OSL data and a unique second-order fit equation ($s = 278 \times 10^3$ counts Gy^{-1} and $a = 22.5 \times 10^3$ counts Gy^{-2}).

Table 1. Fit parameters for calibration curves.

Electron energy	9 MeV	12 MeV	18 MeV
s (10^3 counts Gy^{-1})	276.8 ± 0.5	277.6 ± 0.5	278.1 ± 0.5
a (10^3 counts Gy^{-2})	21.9 ± 0.5	23 ± 0.5	22.3 ± 0.5

equation:

$$aD^2 - sD + I_{OSL} = 0 \quad (1)$$

where s is the slope (in counts Gy^{-1}), I_{OSL} the integrated OSL signal (counts) and a the second-order coefficient (in counts Gy^{-2}). The line of linearity is the derivative of the calibration curve (at $D = 0$ Gy).

The (physical) solution of Equation (1) is:

$$D\,(\mathrm{Gy}) = \frac{s}{2a}\left(1 - \sqrt{1 - \frac{4aI_{OSL}}{s^2}}\right) \quad (2)$$

A second-order Taylor-series expansion may be used for Equation (2) up to 0.5 Gy (0.3% error). The observed change in slope versus electron energy is very small ($\pm 0.25\%$) and the second-order coefficients do not depend on electron energy within the experimental uncertainties (Table 1). Indeed, at z_{ref}, the average electron energies impinging onto the Al_2O_3 crystal are about 6.5, 5.3 and 4.3 MeV for 18, 12 and 9 MeV, respectively. Since the Al_2O_3 crystal is small (millimetre) with respect to particle ranges (centimetres), the dose is mostly deposited by electrons coming from crystal surroundings (polymers, water) according to Bragg-Gray principle. The dose correction factor D_{Al2O3}/D_{water} involves relative mass collision stopping power[15] of Al_2O_3 to that of water. A rough estimate shows that its energy dependence is indeed very small ($\pm 0.2\%$ in the same energy range). To illustrate this, only one energy independent fit curve is used and the residuals between OSL data and the fit curve are plotted as shown in Figure 5 (bottom).

Depth–dose measurements

The sensor arrangement was moved inside the water, along the central axis of the beam, at different depths according to electron energy. Integrals of OSL signals measured during DD measurements were then converted into absorbed doses using Equation (2) and compared with reference dose data (IC). Figure 6 shows the fairly good agreement ($\pm 0.9\%$) between measured and reference DD data for the three reference energies. This result may be compared with other uncertainties obtained in similar conditions (*i.e.* multiple use of a single detector): $\pm 0.7\%$[4]; $\pm 0.6\%$[3]; $\pm 0.5\%$[7] at 1 Gy; $\pm 2.5\%$[5] at 0.5 Gy.

The OSL sensor, PMMA tube and water phantom have been modelled with the MCNP5 code (Monte-Carlo N-Particles, Los Alamos National Laboratory, NM, USA). The detection volume (mm^3) is small with respect to the global experiment (accelerator and cube phantom). In order to save calculation time, the LINAC beam was modelled by three simplified phase-space files involving a parallel electron beam, emitted from a homogeneous square field of $10 \times 10\,cm^2$. Gaussian distributions in energy were adjusted to fit experimental data in the deepest part of the DD curve. E is the average energy and a, the width of the distribution. The full-width at half-maximum (FWHM) is $2a\sqrt{\ln 2}$. The *f8 mode (p, e) was used.

CONCLUSIONS

In the context of an increasing demand for quality assurance of the dose in RT, Al_2O_3:C-based OSL film dosimetry is gaining wide acceptance among medical physicists with the purpose of performing *in vivo* dose measurements. However, on-line *in vivo* dosimetry is requested for by the medical community in order to provide a quick assessment of delivered doses and to take suitable remedial actions in necessary clinical conditions. Al_2O_3–OSL fibre sensors are potentially attractive for this purpose.

For the purpose of cost-effectiveness and easier data handling, the CEA LIST has designed an innovative multichannel OSL fibre reader. TLD_{500} alumina fibre crystals were used as OSL detectors. The fading of OSL signal is small ($\sim -1\%$ per decade) and no transient effect is observed.

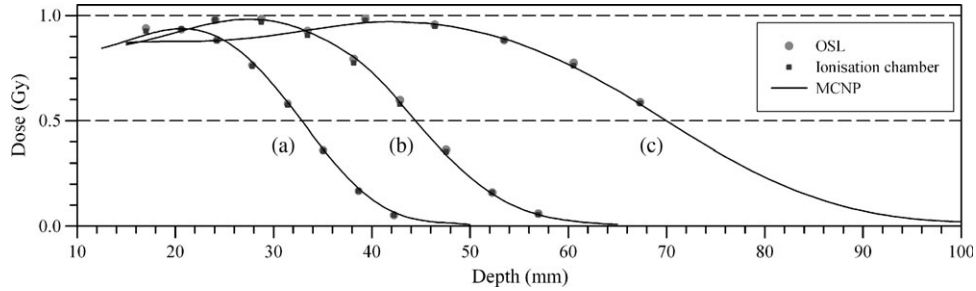

Figure 6. Comparison between central-axis depth–dose curves obtained from optically stimulated luminescence sensor and ionisation chamber. Continuous drawings are Monte-Carlo modellings obtained from simplified phase-space files [field size: 10×10 cm^2, Gaussian distribution: (a) $E = 8$ MeV, full width half maximum (FWHM) = 2.16 MeV; (b) $E =$ 10.4 MeV, FWHM = 2.66 MeV; (c) $E = 16$ MeV, FWHM = 5.5 MeV].

A reproducible readout procedure should reduce fading-induced uncertainty. OSL also depends on both irradiation and stimulation temperatures. The sensitivity is minimum (0.16% K^{-1}) when OSL stimulation is performed at constant temperature.

The repeatability of the OSL dosemeter mainly depends on stability of both the predosed OSL sensors and MC (mainly the optical switch). It was evaluated in preclinical conditions at IGR under multichannel operation (four sensors) with photon beams. It is satisfactory (between 0.6 and 1.3%) and not affected by repeated connections and disconnections. The repeatability was also evaluated using high-energy electron beams in reference conditions. Sensor calibration and DD measurements were performed with a Saturne 43 LINAC at CEA LIST LNHB. Calibration curves show a sublinear behaviour accurately fitted by an energy-independent second-order equation [in the range (9–18 MeV)]. The difference between absorbed doses measured by OSL and the IC is $\pm 0.9\%$ for 1 Gy.

All these results confirm that Al_2O_3:C OSL fibre sensors and multichannel reader approach have great potential for achieving *in vivo* on-line dosimetry in RT. Further tests in pre-clinical conditions at IGR facilities, checking the compliance of the system and software with respect to medical specifications, will be reported.

ACKNOWLEDGEMENTS

S. Magne would like to thank D. Chambellan for his assistance with the X-ray generator, S. Sorel and A. Ostrowsky for their assistance with the LINAC, O. Gal, A. Fallet and G. Bouhot for MCNP modellings.

FUNDING

This work is done in the framework of both French CODOFER Project (*Agence Nationale de la Recherche-Technologie pour la Santé*, www.tecsan.cea.tr) and European Integrated Project CE503564 MAESTRO (Methods and Advanced Equipments for the Simulation and Treatment in Radio Oncology, www.maestro-research.org) of the Sixth Framework Programme, granted by the European Commission.

REFERENCES

1. International Atomic Energy Agency. *Absorbed dose determination in external beam radiotherapy: An international Code of Practice for dosimetry based on standards of absorbed dose to water*. IAEA TRS 398, Vienna, Austria (2000).
2. Schembri, V. and Heijmen, B. J. M. *Optically stimulated luminescence (OSL) of carbon-doped aluminum oxide (Al_2O_3:C) for film dosimetry in radiotherapy*. Med. Phys. **34**, 2113–2118 (2007).
3. Jursinic, P. A. *Characterization of optically stimulated luminescent dosimeters, OSLDs, for clinical dosimetric measurements*. Med. Phys. **34**, 4594–4604 (2007).
4. Yukihara, E. G., Mardirossian, G., Mirzasadeghi, M., Guduru, S. and Ahmad, S. *Evaluation of Al_2O_3:C optically stimulated luminescence (OSL) dosimeters for passive dosimetry of high-energy photon and electron beams in radiotherapy*. Med. Phys. **35**, 260–269 (2008).
5. Viamonte, A., da Rosa, L. A. R., Buckley, L. A., Cherpak, A. and Cygler, J. E. *Radiotherapy dosimetry using a commercial OSL system*. Med. Phys. **35**(4), 1261–1266 (2008).
6. Akselrod, M. S., Botter-Jensen, L. and McKeever, S. W. S. *Optically stimulated luminescence and its use in medical dosimetry*. Radiat. Meas. **41**, S78–S99 (2007).
7. Aznar, M. C., Andersen, C. E., Botter-Jensen, L., Bäck, S. A. J., Mattsson, S., Kjaer-Kristoffersen, F. and Medin, J. *Real-time optical fibre luminescence dosimetry for radiotherapy: physical characteristics and applications in photon beams*. Phys. Med. Biol. **49**, 1655–1669 (2004).
8. Marckmann, C. J., Andersen, C. E., Aznar, M. C. and Botter-Jensen, L. *Optical fibre dosemeter systems for clinical applications based on radioluminescence and optically stimulated luminescence from Al_2O_3:C*. Radiat. Prot. Dosim., **120**, 28–32 (2006).

9. Magne, S., Auger, L., Isambert, A., Bridier, A., Ferdinand, P. and Barthe, J. *Multichannel fibre optic dosimeter based on OSL for dose verification during radiotherapy treatments.* In: Proceedings of the SPIE 6619, Third European Workshop on Optical Fibre Sensors (EWOFS), Cutolo, A., Culshaw, B. and Lopez-Higuera, J. M., Eds. (Napoli, Italy), pp. 1N1–1N4 (2007)
10. Ranchoux, G., Magne, S., Bouvet, J. P. and Ferdinand, P. *Fibre remote optoelectronic gamma dosimetry based on optically stimulated luminescence of Al_2O_3:C.* Radiat. Prot. Dosim., **100**, 255–260 (2002).
11. Magne, S., Ranchoux, G. and Bouvet, J. P. French Patent 2,826,733, EP 1,273,931, US 6,998,632.
12. Edmund, J. M. and Andersen, C. E. *Temperature dependence of the Al_2O_3:C response in medical luminescence dosimetry.* Radiat. Meas. **42**, 177–189 (2007).
13. Edmund, J. M., Andersen, C. E., Marckmann, C. J., Aznar, M. C., Akselrod, M. S. and Botter-Jensen, L. *CW-OSL measurement protocols using optical fibre Al_2O_3:C dosemeters.* Radiat. Prot. Dosim. **119**, 368–374 (2006).
14. Yukihara, E. G., Whitley, V. H., McKeever, S. W. S., Akselrod, A. E. and Akselrod, M. S. *Effect of high-dose irradiation on the optically stimulated luminescence of Al_2O_3:C.* Radiat. Meas. **38**, 317–330 (2004).
15. ESTAR database. Available on www.physics.nist.gov/PhysRefData/Star/Text/contents.html